THE JOURNAL OF BIOLOGICAL CHEMISTRY VOL. 280, NO. 41, pp. 34946–34955, October 14, 2005

Modification of the Structure and Function of Fibrillin-1 by Homocysteine Suggests a Potential Pathogenetic Mechanism in Homocystinuria*

Received for publication, April 29, 2005, and in revised form, July 27, 2005 Published, JBC Papers in Press, August 11, 2005, DOI 10.1074/jbc.M504748200

Dirk Hubmacher[‡§], Kerstin Tiedemann[‡], Rainer Bartels[¶], Jürgen Brinckmann[‖], Tillman Vollbrandt[§], Boris Bätge[**], Holger Notbohm[§], and Dieter P. Reinhardt[‡‡§1]

*From the [‡]Faculty of Medicine, Department of Anatomy and Cell Biology and [‡‡]Faculty of Dentistry, McGill University, Montreal, Quebec H3A2B2, Canada, the Departments of [§]Medical Molecular Biology and [‖]Dermatology, University of Lübeck, 23538 Lübeck, Germany, the [¶]Forschungszentrum Borstel, 23845 Borstel, Germany, and the **Klinikum Neustadt, 23730 Neustadt, Germany*

Homocystinuria, a disorder originating in defects in the methionine metabolism, is characterized by an elevated plasma concentration of homocysteine. Most patients have a defect in the cystathionine-β-synthase, the key enzyme in the conversion of homocysteine to cysteine. Many abnormalities in the connective tissue of patients with homocystinuria resemble those seen in Marfan syndrome, caused by mutations in fibrillin-1. These observations led to the hypothesis that the structure and function of fibrillin-1 is compromised in patients with homocystinuria. To test this hypothesis we produced recombinant human fibrillin-1 fragments spanning the central portion of the molecule (8-Cys/transforming growth factor-β binding domain 3 to calcium binding EGF domain 22) and extensively analyzed the potential of homocysteine to modify structural and functional properties of these proteins. Circular dichroism spectroscopy revealed moderate changes of their secondary structures after incubation with homocysteine. Equilibrium dialysis demonstrated a number of high affinity calcium binding sites in the tandemly repeated calcium binding epidermal growth factor-like domains 11–22. Calcium binding of homocysteine-modified fragments was completely abolished. Incubation of the recombinant proteins with homocysteine rendered the analyzed calcium binding EGF domains as well as the 8-Cys/transforming growth factor-β binding domain 3 significantly more susceptible to proteolytic degradation. Furthermore, data were obtained demonstrating that homocysteine can covalently modify fibrillin-1 via disulfide bonds. These data strongly suggest that structural and functional modifications as well as degradation processes of fibrillin-1 in the connective tissues of patients with homocystinuria play a major role in the pathogenesis of this disorder.

Fibrillin-1 together with fibrillin-2 and -3 constitute a family of large (350 kDa) calcium binding (cb)[2] extracellular matrix proteins which form the backbone of the 10–12-nm-diameter microfibrils (1–3). The spectrum of physiological functions of microfibrils is versatile. It is believed that they serve as a scaffold for the deposition of elastin and, thus, for the correct formation of the elastic fibers (4). In the eye microfibrils are the major component of the ciliary zonules holding the lens in the correct position. Microfibrils are also suggested to play a role in the regulation of morphogenic substances like transforming growth factor β (TGF-β) through the interaction of fibrillin-1 with latent TGF-β-binding proteins (5). Fibrillins display a pronounced modular protein design characterized by an unusual high (12–13%) overall content of cysteine residues. The majority of these cysteine residues are predicted to be involved in intramolecular disulfide bonds stabilizing individual domains (6–8). The most prominent domains are the epidermal growth factor-like (EGF) domain and the 8-Cys/TB domain, characterized by 3 and 4 stabilizing disulfide bonds, respectively. 42–43 of the 46–47 EGF like domains are of the calcium binding type (cbEGF) (9).

Calcium binding to cbEGF domains in fibrillins is essential for stabilization of a rod-like structure (6, 10), for the resistance against proteases (11–14), and for the interaction with ligands such as heparan sulfate, MAGP-1, or fibulin-2 (15–17). Calcium binding to cbEGF domains is mediated by the consensus sequence (D/N)*X*(D/N)(E/Q)X_m(D/N)X_n (Y/F) in the N-terminal part of the domain (9). In contrast to isolated cbEGF domains with dissociation constants in the millimolar range, the affinity for calcium of tandemly repeated cbEGF domains is typically higher (~0.35–500 μM), indicating a stabilizing effect of the surrounding domains (18–23). The calcium concentration in extracellular environments is predicted to be about 1–2 mM. High affinity calcium binding sites are, thus, expected to be fully saturated, whereas low affinity binding sites are likely only partially saturated, which may be important for the regulation of flexibility, elastic properties, degradation, and/or protein-protein interactions.

Mutations in fibrillin-1 lead to the autosomal dominant disorder Marfan syndrome (MIM 154700), which is characterized by symptoms in the cardiovascular, the skeletal, and the ocular systems (24). Most currently known mutations (72%) leading to Marfan syndrome are point mutations, and about 35% of all mutations generate or substitute cysteine residues (25). A number of these mutations make fibrillin-1 more susceptible for protease digestion, most likely by inducing subtle structural changes in close vicinity of the affected amino acid residue (11–14). Mutations in the center of the molecule (exons 24–32) often lead to the very severe neonatal form of Marfan syndrome (for review, see Ref. 26).

Homocystinuria (MIM 236200) is an autosomal recessive disorder originating from enzymatic defects of the methionine metabolism. The major cause of homocystinuria is a deficiency in the cystathionine-β-synthase, an enzyme involved in the conversion of homocysteine to cysteine (27). This deficiency leads to significantly elevated plasma con-

* This work was supported by Canadian Institutes of Health Research Grant MOP-68836, the Deutsche Forschungsgemeinschaft Grant SFB367-A1, and the German Academic Exchange Service (postdoctoral fellowship to D. H.). The costs of publication of this article were defrayed in part by the payment of page charges. This article must therefore be hereby marked "*advertisement*" in accordance with 18 U.S.C. Section 1734 solely to indicate this fact.

[1] To whom correspondence should be addressed: Dept. of Anatomy and Cell Biology, McGill University, Montreal, Quebec H3A 2B2, Canada. Tel.: 514- 398-4243; Fax: 514-398-5047; E-mail: dieter.reinhardt@mcgill.ca.

[2] The abbreviations used are: cb, calcium binding; EGF, epidermal growth factor-like; FITC, fluorescein isothiocyanate; Hcy, homocysteine; Hcy-FITC, homocysteine-labeled FITC; Hcy-Tris, homocysteine-labeled Tris; TCEP, Tris(2-carboxyethyl)phosphine hydrochloride; TBS, Tris-buffered saline.

centrations of the toxic amino acid homocysteine of up to 500 μM compared with 10 μM under normal conditions (28, 29). The most prominent clinical symptoms of patients with homocystinuria are mental retardation, ectopia lentis, skeletal abnormalities, and vascular disease (27). The skeletal and ocular symptoms resemble the symptoms seen in patients with Marfan syndrome, and in both disorders histopathological findings included fragmented elastic fibers in the aortic wall (27, 30). Although the genetic cause for homocystinuria has been determined, it is not clear how elevated levels of homocysteine lead to the pathogenetic mechanisms. We and others hypothesized that due to the reductive potential of homocysteine, it may be able to chemically modify the structure of the heavily disulfide-bonded fibrillin-1 and, thus, alter its functional properties.

Only a few studies addressed the molecular consequences of elevated homocysteine levels on extracellular matrix proteins including fibrillins. In a high methionine diet chick model with elevated homocysteine levels, the amounts of fibrillin-2 and elastin-associated microfibrils in the aortic wall were reduced (31). Analysis of smooth muscle cells showed no negative influence of elevated homocysteine concentrations on fibrillin-1 deposition in the extracellular matrix (32). However, reduced cysteine concentrations, which are also found in patients with homocystinuria, decreased the amount of fibrillin-1 deposited into the matrix (32). It has been shown for other cbEGF domain-containing proteins such as thrombomodulin or protein C that homocysteine can inactivate these proteins (33). Recently, it was reported that homocysteine modifies the structure of procaryotically expressed fibrillin-1 and Notch1 fragments by reshuffling of disulfide bonds and covalent binding of homocysteine to cbEGF domains (34).

Here, we demonstrate that homocysteine in concentrations found in patients with homocystinuria lead to structural modifications of recombinant human fibrillin-1 fragments and loss of calcium binding. These molecular alterations lead to enhanced protease sensitivity. Based on these data, we suggest that degradation of fibrillin-1 in the connective tissues of patients with homocystinuria plays a major role in the pathogenesis of this disorder.

EXPERIMENTAL PROCEDURES

Expression Constructs—The following three expression constructs for human fibrillin-1 fragments were designed with hexahistidine tags at the C-terminal end which were introduced with appropriate antisense primers for the respective PCR to facilitate protein purification. Due to the cloning strategy, all sequences are preceded at the N-terminal end by Ala-Pro-Leu-Ala. The template for PCR was cDNA clone HFBN8 (35). To generate the expression plasmid for rF1B coding for Asp^{952}—Val^{1196}, the 766-bp NheI-XhoI-restricted PCR product generated with oligonucleotides 5′-ATCGTAGCTAGCTGATATCCGCCTGGAAACCTGC-3′ and 5′- ACCGAACTCGAGCTATTAGTGATGGTGATGGTGATGAACACAAAATAGCCTATCGGGAG-3′ was subcloned into the NheI-XhoI-restricted pDNSP-rF51 (14), resulting in plasmid pDNSP-rF1B. The expression plasmid for rF1C coding for Asp^{1197}–Thr^{1362} (pDNSP-rF1C) was produced by subcloning the 529-bp NheI-XhoI-restricted PCR fragment amplified with 5′-ATCGTAGCTAGCTGACATTGATGAATGCAGCATAATG-3′ and 5′- ACCGAACTCGAGCTATTAGTGATGGTGATGGTGATGAGTGCACTTAATGCCATCTCC-3′ into the NheI-XhoI-restricted pDNSP-rF51. To produce the expression plasmid for rF1D coding for Asp^{1363}–Val^{1527}, the 530-bp NheI-ApaI PCR fragment generated with 5′-ATCGTAGCTAGCTGATCTGGACGAATGTTCCAATGG-3′ and 5′- AATTAAGGGCCCTATTAGTGATGGTGATGGTGATGAACACAGCCAACTCGAGTTGGG-3′ was fused with the NheI-ApaI-restricted pDNSP-rF51, resulting in a plasmid termed pDNSP-rF1D. The correct sequence of all expression plasmids was verified by commercial DNA sequencing (Agowa, Berlin).

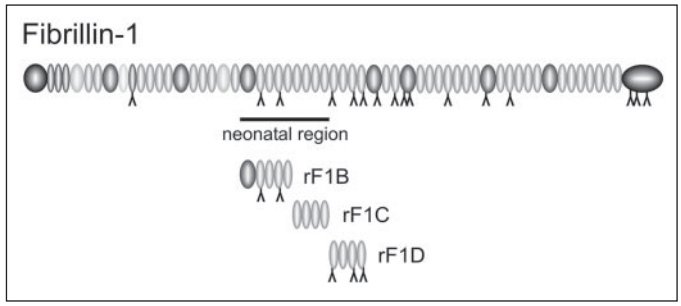

FIGURE 1. **Schematic overview of the recombinant fibrillin-1 fragments rF1B, rF1C, and rF1D.** This overview shows the relative position of the expressed fragments of human fibrillin-1 used in this study. The 3 fragments span subsequent parts of the region between 8-Cys/TB domain 3 and cbEGF domain 22. Fragments rF1B and rF1C comprise the neonatal region of fibrillin-1 (*bar*). Each of the recombinant fragments contains four cbEGF domains. The predicted *N*-linked glycosylation sites are indicated (*inverted Y*).

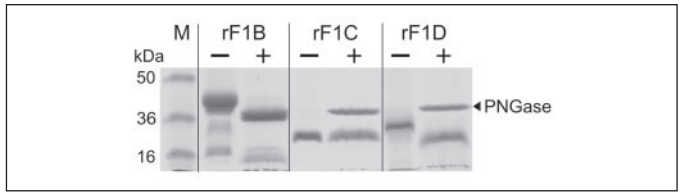

FIGURE 2. **Characterization of the *N*-linked glycosylation of recombinant fibrillin-1 fragments.** Recombinantly expressed fibrillin-1 fragments rF1B (10 μg), rF1C (5 μg), and rF1D (10 μg) were analyzed by reducing (20 mM dithiothreitol) SDS gel electrophoresis before (−) and after (+) treatment by *N*-glycosidase F (*PNGase*). The position of the *N*-glycosidase F (~36 kDa) is indicated by the *arrowhead*. The masses of globular marker proteins (*M*) are indicated.

Transfection of Cells and Culture Conditions—Human embryonic kidney cells (293, American Type Culture Collection) were transfected with the PvuI-linearized expression plasmids described above using calcium phosphate as described (36). The cells were grown in Dulbecco's modified Eagle's medium (PAA Laboratories) supplemented with 2 mM glutamine, 100 units/ml penicillin, 100 μg/ml streptomycin, and 10% fetal calf serum in a 5% CO_2 atmosphere at 37 °C. Selection of recombinant clones started after 24 h with 0.25 mg/ml G418. Single colonies were isolated and propagated. Positive clones were identified by Western blotting and detection with an antibody directed against the hexahistidine tag (Invitrogen).

Production and Purification of the Recombinant Polypeptides—Recombinant cell clones were grown in triple-layer flasks (Nalge Nunc International), and serum-free medium was collected every 2–3 days and stored at −20 °C. After thawing 2–3 liters of conditioned medium containing rF1B, rF1C, or rF1D, phenylmethylsulfonyl fluoride was supplemented to a final concentration of 0.1 mM. The medium was concentrated to ~50 ml by ultrafiltration (10-kDa cutoff), dialyzed against 20 mM HEPES, 500 mM NaCl, pH 7.2, and loaded on a 1-ml HiTrap chelating column charged with Ni^{2+} (GE Healthcare). The bound histidine-tagged proteins were eluted with a gradient of 0–500 mM imidazole in the same buffer in 40 ml at a flow rate of 1 ml/min. Fractions containing the protein of interest were pooled, dialyzed against 50 mM Tris-HCl, 150 mM NaCl, pH 7.4 (TBS) containing 2 mM $CaCl_2$, and stored at −80 °C.

Recombinant rF1D bound relatively weakly to the Ni^{2+}-chelating column, and much of the material was found in the flow-through. Therefore, the flow-through after Ni^{2+}-chelating chromatography was dialyzed against 20 mM Tris-HCl, 50 mM NaCl, pH 8.6, and loaded on a

TABLE ONE

Characterization of N-linked glycosylation of rF1B, rF1C, and rF1D

	rF1B	rF1C	rF1D
Calculated molecular mass (kDa)	28.6	18.9	18.9
Determined molecular mass (kDa)	38.3	31.5	33.6
Determined molecular mass after *N*-glycosidase F digestion (kDa)	35.7	31.5	31.5
Determined *N*-linked oligosaccharides (%)[a]	6.8	0	6.3
Predicted *N*-glycosylation sites	2	0	3
Predicted *O*-glycosylation sites[b]	0	0	0

[a] The percentages represent the percentage of total mass as determined by SDS gel electrophoresis shown in Fig. 2.
[b] The absence of mucin type *N*-acetylgalactosamine *O*-glycosylation sites was predicted using the NetOGlyc server (43).

HiTrap Q anion exchange column (GE Healthcare) equilibrated in the same buffer. Bound proteins were eluted with a linear gradient (15 ml) of equilibration buffer containing 50–1000 mM NaCl at a flow rate of 0.5 ml/min. The fractions containing rF1D were pooled, concentrated to <1 ml, and loaded on a Superose 12 gel filtration column (24 ml; GE Healthcare) equilibrated with TBS containing 2 mM $CaCl_2$. Recombinant rF1D eluted between 11 and 13 ml. The quality of all protein preparations was evaluated by SDS-PAGE, and the identity of each protein was verified by N-terminal sequencing.

Homocysteine Preparation—A 30 mM stock solution of homocysteine was prepared from homocysteine-thiolactone (Fluka) according to the procedure of Duerre and Miller (37) with minor modifications. Briefly, 46.11 mg of homocysteine-thiolactone were dissolved in 0.3 ml of 5 N NaOH and incubated for 5 min at room temperature. About 1.5 ml of 1 M KH_2PO_4 was added to adjust the final pH to 7.0. After the addition of 8 ml of H_2O (final calculated homocysteine concentration = 30 mM), an aliquot was removed to determine the absolute concentration of free homocysteine. This was performed with Ellman's reagent (Pierce) according to the manufacturer's instructions (38). Homocysteine aliquots were stored at −80 °C and thawed only once. Determination of the homocysteine concentration after 1 month indicated no substantial loss of free homocysteine.

Incubation of Recombinant Proteins with Homocysteine—To mimic the exposure of fibrillin-1 to elevated homocysteine levels found in patients with homocystinuria, recombinant fragments of fibrillin-1 in TBS containing 2 mM $CaCl_2$ were incubated with 300 μM homocysteine for 24 h at 37 °C. Due to the short half-life of homocysteine in solution (~2 h), a second 300 μM aliquot was added to the proteins after 12 h.

Calcium Binding Studies—To remove calcium from either the non-treated or the homocysteine-modified fragments dissolved in TBS containing 2 mM $CaCl_2$, the samples were supplemented with 10 mM EDTA and incubated for 1 h at ~20 °C and then dialyzed for 24 h against TBS in the presence of 5 g/100 ml Chelex-100 (Bio-Rad). The dialysis buffer was changed 4 times, and the last buffer volume was filtered to retain the Chelex-100 resin and used as calcium-free TBS to prepare calcium stock solutions and to adjust the protein concentration of calcium-free recombinant proteins. Equilibrium dialysis was performed with DispoEquilibrium Dialyzers (Harvard Apparatus) equipped with a membrane with a molecular weight cutoff of 1000. 50 μl of protein solution in calcium-free TBS was dialyzed against 50 μl of 0.05–2 mM $CaCl_2$ in TBS including trace amounts of $^{45}Ca^{2+}$ (PerkinElmer Life Sciences). After dialysis for 24 h at 37 °C, 2–3 15-μl aliquots were counted in a scintillation counter (WinSpectral α/β 1414, Wallac). For curve fitting, equal and independent binding sites were assumed using the fitting function [bound Ca^{2+}]/[recombinant fragment] = $n \times$ [free Ca^{2+}]/($K_{d\ \mathrm{average}}$ + [free Ca^{2+}]), where n = the number of binding sites, and $K_{d\ \mathrm{average}}$ = the average thermodynamic dissociation constant. To verify that the hexahistidine tags on the C-terminal end of the proteins did not contribute to calcium binding, a control protein (main proteinase from the severe acute respiratory syndrome virus) containing a hexahistidine tag was tested under identical conditions by calcium equilibrium dialysis. This control protein did not bind calcium.

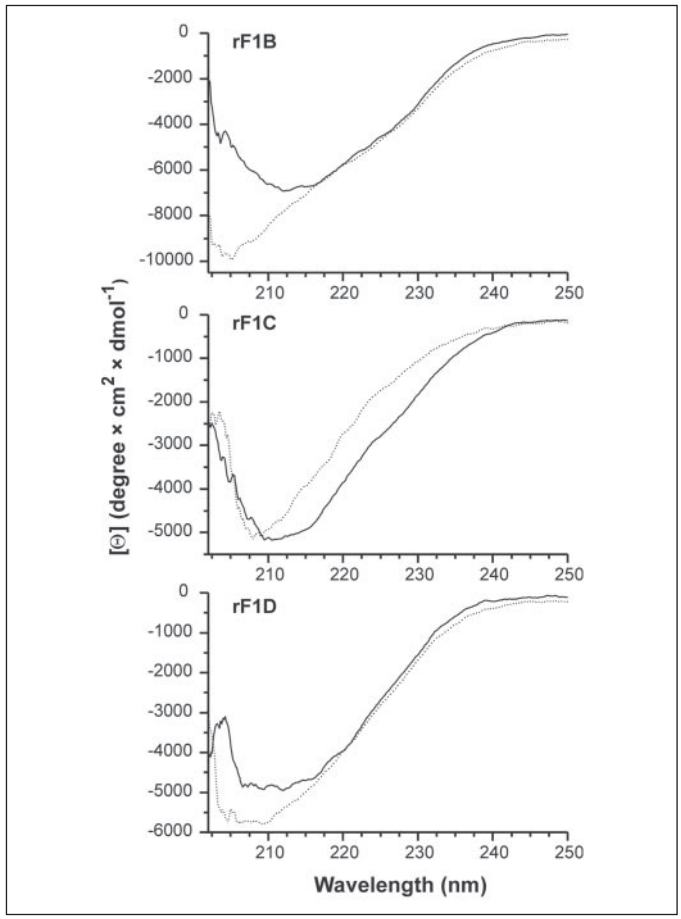

FIGURE 3. **Secondary structure analysis by CD spectroscopy.** Far-UV circular dichroism spectra of rF1B, rF1C, and rF1D (0.5 mg/ml each) were recorded at 20 °C. Non-treated fragments (*solid lines*) and homocysteine-treated fragments (*dotted lines*) were analyzed in the presence of 10 mM $CaCl_2$ in TBS buffer. Curves represent the means of three independent experiments. Measurements below 202 nm are not shown due to the strong absorption of the buffer. The mean residue ellipticity [Θ] is blotted against the wavelength in nm.

Protease Degradation Experiments—The unmodified or homocysteine-modified recombinant fibrillin-1 fragments rF1B, rF1C, and rF1D were incubated in the presence or absence of 6.25–9.5 mM $CaCl_2$ in TBS with trypsin (E.C. 3.4.21.4, Sigma) or α-chymotrypsin (E.C. 3.4.21.1, Sigma) for up to 16 h. After removing a control sample at time 0, the enzymes were added in a ratio of 1:40 (w/w) and incubated at 30 °C

TABLE TWO

Secondary structure analysis from circular dichroism spectra of recombinant non-treated and homocysteine-treated fibrillin-1 fragments

	rF1B		rF1C		rF1D	
	Non-treated	Hcy-treated	Non-treated	Hcy-treated	Non-treated	Hcy-treated
α-Helix	0.10	0.16	0.07	0.08	0.08	0.09
β-Sheets	0.36	0.29	0.37	0.35	0.36	0.34
β-Turns	0.22	0.23	0.22	0.22	0.22	0.22
Other	0.32	0.33	0.34	0.36	0.35	0.35
Total[a]	1.00	1.01	1.00	1.01	1.01	1.00

[a] Values were calculated using the ContinLL method (39, 40).

(chymotrypsin) or 37 °C (trypsin) as instructed by the supplier. Samples were removed after 0.5, 1, 2, and 16 h and immediately transferred into reducing 4-fold concentrated sample buffer, heated to 95 °C for 5 min, and chilled on ice until all samples were collected for analysis by SDS gel electrophoresis (15% acrylamide (w/v)). The protein fragments were stained with Coomassie Brilliant Blue.

N-terminal Sequencing—To determine the amino acid sequence of the recombinant proteins and the protease degradation products, the fragments were separated by reducing (20 mM dithiothreitol) SDS gel electrophoresis, blotted on a polyvinylidene difluoride membrane (Immobilon P, Millipore), and stained with Coomassie Brilliant Blue. The fragments of interest were cut out and directly sequenced with an automated protein sequencer (Model Procise 494, Applied Biosystems). For identification of the N-terminal amino acid in each sequencing cycle, it was reacted with phenylisothiocyanate, removed as an anilinothiazoline derivative, converted to the more stable phenylthiohydantoin-amino acid (PTH-AA), separated by a high performance liquid chromatography gradient system, and compared with an external standard mixture of known PTH-AAs.

Circular Dichroism (CD) Spectroscopy—The CD spectra of the recombinant unmodified and homocysteine-modified fibrillin-1 fragments (0.5 mg/ml in TBS) were recorded in the presence of 10 mM $CaCl_2$. Homocysteine-treated samples were extensively dialyzed before the analysis to remove free homocysteine. The samples were analyzed in quartz cuvettes on a Jasco J-175 instrument. Spectra were recorded from 200 to 250 nm at 20 °C. Secondary structure analysis was performed with the ContinLL method (39, 40).

Labeling of Homocysteine and Immunofluorescence—For labeling of homocysteine with fluorescein isothiocyanate (FITC), 100 μl of FITC (5 mg/ml in Me_2SO) was added in 5-μl aliquots to 1 ml of 19 mM homocysteine in Tris-HCl, pH 7.0. The reaction mixture was incubated at 4 °C for 8 h in the dark. To stop the reaction, 12 μl of 5 M NH_4Cl was added. The FITC-labeled homocysteine (Hcy-FITC) was sterile-filtrated and stored at −80 °C. As a control, Tris-HCl was labeled in an identical fashion (Tris-FITC).

For immunofluorescence, normal human dermal fibroblasts (passage 8–9) were prepared as described in detail previously (36). Briefly, cells were trypsinized and seeded at densities of 7.5×10^4 cells/well in 8-well chamber slides (Permanox; Nalge Nunc International) resulting in a confluent cell layer after attachment of the cells. The cells were grown in Dulbecco's modified Eagle's medium containing 10% (v/v) fetal calf serum in the presence of Hcy-FITC or Tris-FITC at a final concentration of 300 μM. The medium was changed daily, and 2–4 days after seeding the cells were fixed with 70% (v/v) methanol/30% (v/v) acetone and either visualized directly with an Axioskop2 microscope (Zeiss) or further stained with the polyclonal antiserum α-rF6H reacting with the C-terminal half of fibrillin-1 (15). To reduce potential disulfide bonds between Hcy-FITC and the cysteine residues of fibrillin-1 and other matrix proteins, Tris(2-carboxyethyl)phosphine hydrochloride (TCEP; Sigma) was used in concentrations of 10 mM in phosphate-buffered saline for up to 30 min.

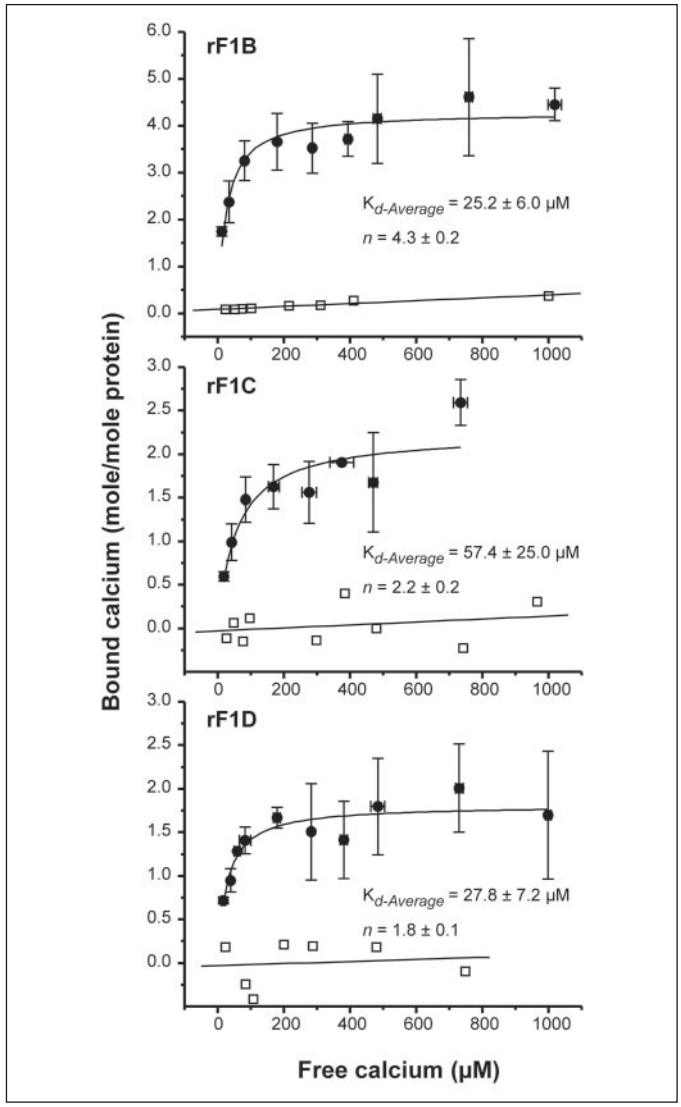

FIGURE 4. **Calcium binding of fibrillin-1 fragments rF1B, rF1C, and rF1D.** Calcium binding of non-treated (*closed circles*) or homocysteine-treated (*open squares*) fibrillin-1 fragments (0.5–1 mg/ml) was analyzed by equilibrium dialysis against increasing concentrations of radioactive-labeled $^{45}CaCl_2$ in TBS buffer. For the non-treated samples, the data points represent the means of three independent experiments including S.D. of the mean. The theoretical curves were calculated as described under "Experimental Procedures." χ^2 values of the curve fittings were 0.1 (rF1B), 0.08 (rF1C), and 0.03 (rF1D). n = the number of binding sites, and $K_{d\ average}$ = the average thermodynamic dissociation constant. For the homocysteine-treated samples, linear curve fitting was applied. Note that homocysteine-treated proteins are not able to bind calcium.

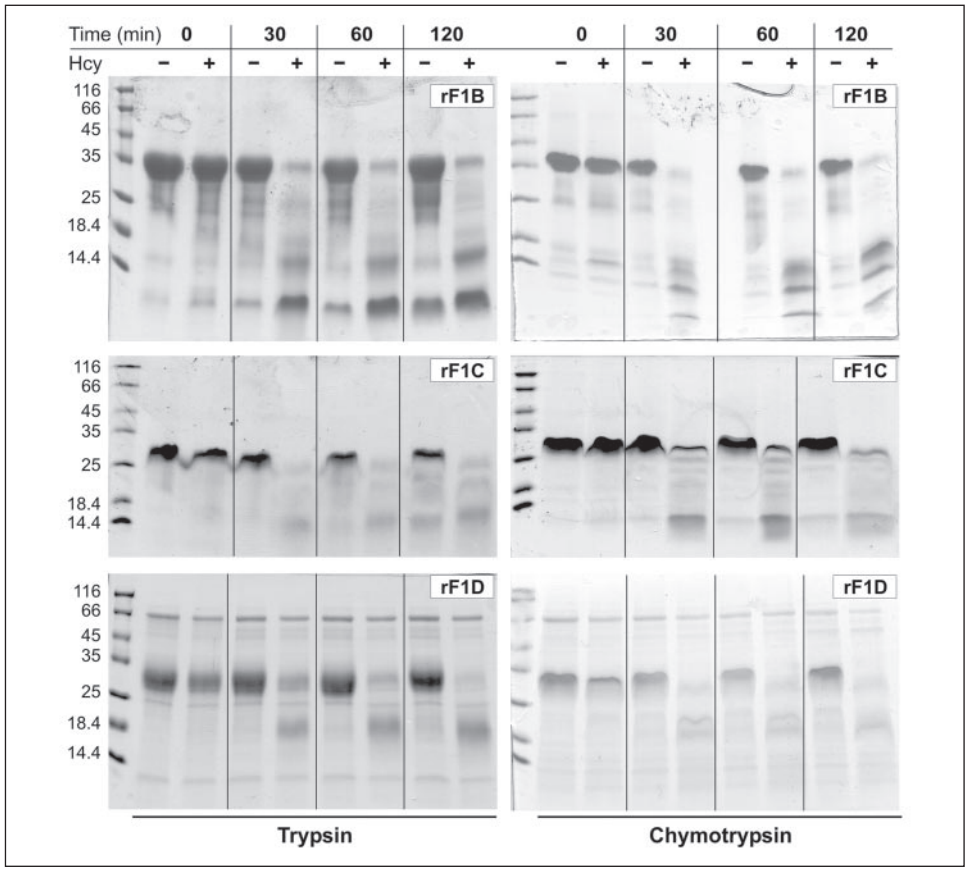

FIGURE 5. **Proteolytic degradation of fibrillin-1 fragments after homocysteine modification.** Non-treated (−) or homocysteine-treated (+) recombinant fragments rF1B, rF1C, and rF1D were incubated with trypsin (*left panel*) or chymotrypsin (*right panel*) for time periods indicated on *top*. Equal amounts of protein (5–20 μg/*lane*) for non-treated and homocysteine-treated proteins were analyzed for each time point. The reaction was stopped by adding an aliquot to reducing SDS-PAGE sample buffer followed by incubation at 95 °C for 5 min. The proteolytic degradation patterns were visualized by SDS gel electrophoresis and Coomassie Blue staining. Positions of reduced marker proteins are indicated on the *left* in kDa.

RESULTS AND DISCUSSION

Although the genetic basis for homocystinuria caused by mutations in enzymes of the methionine metabolism is well characterized, the molecular pathogenetic mechanisms leading to connective tissue abnormalities overlapping with those observed in Marfan syndrome caused by mutations in fibrillin-1 are less well understood. Based on these similar clinical symptoms, we and others hypothesized that homocysteine in elevated concentrations found in individuals with homocystinuria has the potential to modify the structure and function of fibrillin-1. To test this hypothesis, we have produced and characterized recombinant human fibrillin-1 fragments and extensively analyzed the potential of homocysteine modification as well as the structural and functional consequences on the proteins. Because mutations in the so-called neonatal region in the center of the fibrillin-1 molecule (Fig. 1) cause the most severe symptoms in Marfan syndrome, we focused on this and neighboring regions for the analysis of potential homocysteine modifications.

Expression and Properties of Recombinant Human Fibrillin-1 Fragments—The fragments were recombinantly expressed in a well established human embryonic kidney cell system to ensure correct folding and posttranslational modifications. This system has been demonstrated to produce a number of other correctly folded fibrillin-1 fragments (17, 20, 36, 41). The fragments rF1B, rF1C, and rF1D produced here span the region from 8-Cys/TB domain 3 to cbEGF domain 22, representing the longest stretch of 12 tandemly repeated cbEGF domains in fibrillin-1 (Fig. 1). These small recombinant fragments, each containing 4 cbEGF domains, were chosen over previously produced larger fragments to facilitate the analysis and interpretation of the consequences of homocysteine modification on calcium binding and protease susceptibility described below. The recombinant fragments were expressed and secreted into the cell culture medium in amounts of ~2–5 μg/ml/day. The expected N-terminal sequences were verified by Edman degradation.

Fragments rF1B, rF1C, and rF1D contain 2, 0, and 3 potential N-linked glycosylation sites, respectively (Fig. 1). *N*-Linked glycosylation of the recombinant fragments was analyzed by digestion with *N*-glycosidase F (*PNGase F*), an enzyme that cleaves high mannose, hybrid, and complex oligosaccharides from *N*-linked glycoproteins (Fig. 2 and TABLE ONE). rF1B and rF1D showed enhanced mobility in SDS gel electrophoresis after treatment with *N*-glycosidase F but not rF1C. This reduction in the apparent molecular masses of 6.8% for rF1B and 6.3% for rF1D demonstrates that these recombinant fragments are *N*-linked-glycosylated as expected from their primary sequences. These data are in agreement with observations for larger recombinant fragments spanning a similar region in fibrillin-1 (20, 42). No *O*-glycosylation sites in rF1B, rF1C, and rF1D were predicted with the NetOGlyc 3.1 software (43). The molecular masses determined by SDS gel electrophoresis after removal of *N*-linked oligosaccharides were somewhat larger than calculated from the primary sequence (Table I). This property is typical for fibrillin-1 fragments containing a large portion of cysteine residues (20, 44).

Analysis of Secondary Structures by CD Spectroscopy—Far UV CD spectra in the presence of calcium indicate a substantial amount of β-structures for each of the recombinant fragments, which is typical for proteins containing cbEGF domains (Fig. 3) (13, 14, 45). Minima of $\Theta = -6927$ degree $\times$ cm^2 $\times$ dmol^{-1} at 212 nm (rF1B), $\Theta = -5157$ degree $\times$ cm^2 $\times$ dmol^{-1} at 211 nm (rF1C), and $\Theta = -4950$ degree $\times$ cm^2 $\times$ dmol^{-1} at 212 nm (rF1D) were observed. Consistent with previous data obtained with a larger recombinant fibrillin-1 fragment spanning the 8-Cys/TB domain 3 to cbEGF domain 22 (13), the spectra of calcium-free rF1B, rF1C, and rF1D shifted toward lower wavelengths and Θ

TABLE THREE

Susceptible proteolytic cleavage sites in homocysteine-treated fragments rF1B, rF1C, and rF1D, which are normally protected in the non-treated fragments

Fragment	Cleaved sequence[a]	Position[b]	Enzyme[c]
rF1B	L*XX*EDEEC	960	C
	LPIAG*XX*R	969	C/U
	TPEYEE*X*C	1001	C/U
	LC*X*RGPGF	1007	C/U
	FKDINECKMIPSLCT	1026	C
	KDINECKMIPSLCT	1027	C
	MI*X*S*X*CTH	1034	T
	GKCRNT*X*G	1042	C/U
	NCTDIDEC	1067	T
	MKNCMDID	1108	C
	KNCMDIDE	1109	C
	NCMDIDECQRDPLLC	1110	T
	CIDINEC	1153	C/U
rF1C	GGCE*X*FCT	1206	C/U
	SCQPGF	1222	C/U
	ALMPDQ*X*SCTDIDE	1228	C
	SCTDIDECED*X*PN	1235	T
	MASEDM*X*TCVDVNE	1270	C
	TCVD*X*NECDL*X*PN	1277	T
	SGTCE*X*T*X*G	1293	C
	TGCTDINECEIGAH	1318	T
	GCTDINEC	1319	T/U
	HAVC*X*N*X*AGSFKC	1336	T
rF1D	FTC*X*DLDE	1400	C/U
	NLCGNGQC	1413	C
	APGGY*X*CE	1423	T/U
	GTCHNLPG	1459	C
	SGG*X*CTDV	1481	T

[a] Cleaved sequences were determined by Edman degradation of the degradation products and are indicated in the one-letter amino acid code. *X*, residues that could not be identified by N-terminal sequencing. Cysteine residues are shown as C, although they cannot be identified by the procedure used.
[b] Positions are indicated according to Pereira *et al.* (54).
[c] T, trypsin; C, chymotrypsin; in some cases cleavage sites have been observed at positions that are normally not used by trypsin or chymotrypsin (U, unspecific).

values (data not shown). After incubation of all three recombinant fragments with homocysteine in concentrations found in individuals with homocystinuria (300 μM), the spectra differed as compared with the spectra obtained with non-treated proteins (Fig. 3). Homocysteine-treated fibrillin-1 fragments resulted in minima of $\Theta = -9949$ degree $\times$ cm^2 $\times$ dmol^{-1} at 205 nm (rF1B), $\Theta = -5148$ degree $\times$ cm^2 $\times$ dmol^{-1} at 208 nm (rF1C), and $\Theta = -5797$ degree $\times$ cm^2 $\times$ dmol^{-1} at 209 nm (rF1D). Calculating the relative amounts of secondary structure by the ContinLL method (TABLE TWO) showed, as expected, relatively low amounts of α-helix (7–10%), and high amounts of β-sheets (36–37%) and β-turns (22%) for the non-treated proteins. The calculations predicted only small differences in secondary structure between the non-treated and the homocysteine-treated forms.

Based on these data, we suggest that the structural changes observed after homocysteine treatment results from either covalent modification of cysteine residues in fibrillin-1 involved in disulfide-bonds, leading temporarily to free reactive cysteine residues in the protein, or from a rearrangement of disulfide bonds in a reduction-oxidation-like mechanism catalyzed by homocysteine. These interpretations are in agreement with a very recent publication by Hutchinson *et al.* (34) reporting that homocysteine treatment leads to a partial reduction of disulfide bonds in cbEGF domains 32–34 of fibrillin-1 and suggesting that homocysteine initiated disulfide bond shuffling and misfolding of cbEGF domains. Such structural changes would be also reflected on the functional level such as calcium binding.

Calcium Binding of rF1B, rF1C, and rF1D—To determine calcium binding properties, the fibrillin-1 fragments were analyzed by equilibrium dialysis using $^{45}Ca^{2+}$, which allows determining the amount of protein-bound and free calcium at different calcium concentrations (Fig. 4). The average calcium dissociation constant ($K_{d\ \mathrm{average}}$) for rF1B is 25.2 $\pm$ 6.0 μM. For individual cbEGF domains in this region, which are in context with an N-terminally located domain, calcium dissociation constants were reported to be <100 μM (TB3-cbEGF11 (46)), <30 μM for cbEGF13 in the cbEGF12–13 pair (22), or <100 μM for cbEGF14 in the cbEGF13–14 pair (19). Thus, the average dissociation constant for cbEGF11–14 contained in rF1B corresponds well with these data. The average calcium dissociation constants of rF1C ($K_{d\ \mathrm{average}}$ = 57.4 $\pm$ 25.0 μM) and rF1D ($K_{d\ \mathrm{average}}$ = 27.8 $\pm$ 7.2 μM) were in a similar low micromolar range as compared with rF1B. All the fragments contain 4 cbEGF domains which are expected to bind 1 calcium ion each. For rF1B, where the N-terminal cbEGF domain is stabilized by a preceding 8-Cys/TB domain, the number of binding sites (4.3 $\pm$ 0.2) correlated well with the expected value. In rF1C and rF1D, the N-terminal cbEGF domains are not stabilized by preceding domains. N-terminally located cbEGF domains often do not bind calcium efficiently (19, 22, 23). Therefore, 3 calcium binding sites with dissociation constants <1 mM were expected

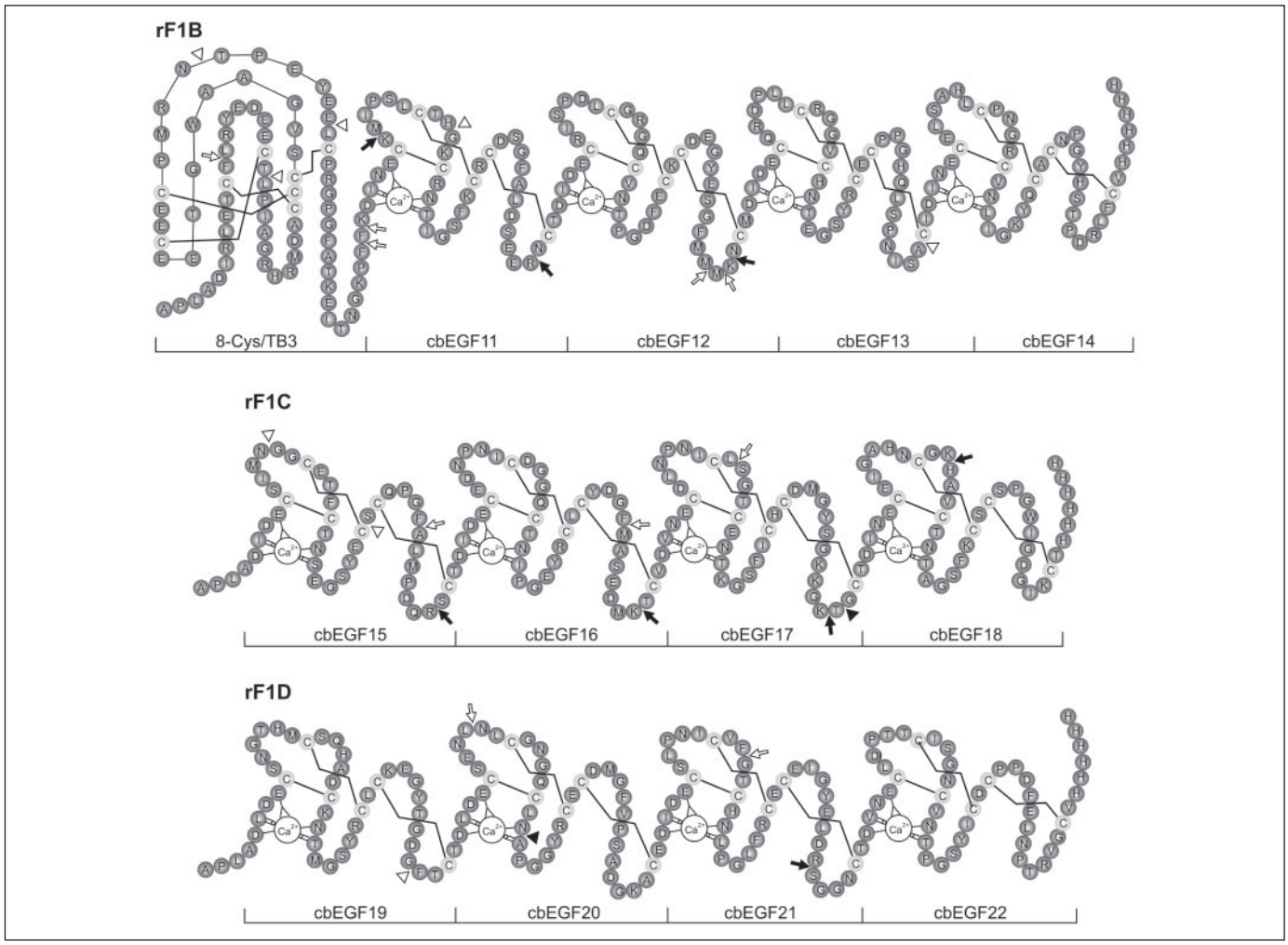

FIGURE 6. **Schematic representation of susceptible proteolytic sites in the fibrillin-1 fragments after treatment with homocysteine.** Sensitive tryptic (*black arrows* and *triangles*) or chymotryptic (*white arrows* and *triangles*) proteolytic cleavage sites, which only were observed after treatment with homocysteine but not or less without treatment (see Table III), are indicated on the polypeptide chain of each recombinant fragment. Typical cleavage sites for each protease are indicated by *arrows*, and non-typical cleavage sites are marked by *triangles*. The two-dimensional projections of the 8-Cys/TB and the cbEGF domain structures were adjusted from references (6, 7). The drawing was generated with the CorelDraw version 11 software.

for rF1C and rF1D. Due to large variations in the results of the equilibrium dialyses at higher calcium concentrations, binding sites with dissociation constants >1 mM could not be analyzed. The number of binding sites observed for rF1C (2.2 ± 0.2) and rF1D (1.8 ± 0.1) were somewhat lower than what was expected based on the domain structure. After removal of calcium by EDTA and Chelex-100, the residual calcium concentration in the buffer system was <0.5 μM. Therefore, the detection of only 2 binding sites in rF1C and rF1D could be due to the presence of 1 very high affinity binding site with dissociation constants below 0.5 μM, from which calcium could not be removed. For cbEGF 22 contained in rF1D, an average dissociation constant of 376 μM was reported previously for a construct containing cbEGF22-TB4-cbEGF23 (20). From the studies presented here it is clear that the calcium dissociation constant of cbEGF 22 is at least 1 order of magnitude lower (*e.g.* the calcium affinity is higher) when this domain is in context with the appropriate N-terminal domains. Similar effects have been observed by others for a number of other cbEGF domains (18, 19, 22, 47).

To test the consequences of homocysteine treatment on the functional ability of the proteins to bind calcium, equilibrium dialyses of homocysteine-treated fragments were performed (Fig. 4). These analyses clearly demonstrate that modification of the fragments with homocysteine in concentrations found in patients with homocystinuria leads to a complete loss of calcium binding for all three fragments. The structural changes observed by CD spectroscopy after treatment with homocysteine are, therefore, sufficient to compromise calcium binding of the recombinant proteins. The consequences of homocysteine on the ability to bind calcium are studied here on cbEGF domain 11–22 of fibrillin-1 contained in the 3 recombinant fragments. It is likely, however, that other cbEGF domains in fibrillin-1 would be similarly affected by treatment with homocysteine. We predict that loss of calcium binding to cbEGF domains of fibrillin-1 after modification with homocysteine plays a critical role in the molecular mechanism leading to homocystinuria. Calcium binding to fibrillin-1 has been demonstrated to be important for ligand binding interactions with ligands such as fibulin-2, MAGP-1, or heparin/heparan sulfate (15–17, 48) or for self-assembly (36, 49). Although these functions are dependent on relatively small epitopes, including one or a few cbEGF domains in the fibrillin-1 molecule, a more general role for calcium was described to protect cbEGF domains from proteolytic degradation (50). Therefore, we tested the consequences of homocysteine modification on proteolytic stability of the fragments.

Proteolytic Degradation of rF1B, rF1C, and rF1D after Modification with Homocysteine—The calcium-loaded recombinant proteins were analyzed before and after treatment with homocysteine for their prote-

ase susceptibility using trypsin and chymotrypsin. In Fig. 5, typical time-resolved degradation patterns for rF1B, rF1C, and rF1D are shown. In general, all three recombinant proteins were considerably more susceptible to proteolytic degradation with trypsin as well as with chymotrypsin. The full-length homocysteine-modified fragments were almost completely degraded to smaller fragments after 30 min of protease incubation, whereas the non-modified fragments were not or only little degraded even after 2 h of protease treatment. Prominent degradation products of homocysteine-treated fragments, which did not occur or occurred significantly less in the non-treated samples, include bands of about 8 and 14 kDa (trypsin) and <10, 14, and 18 kDa (chymotrypsin) for rF1B, bands of 16 and 20 kDa (trypsin) and several bands between 10 and 25 kDa (chymotrypsin) for rF1C, and bands of 18 (trypsin) and 19 and 20 kDa (chymotrypsin) for rF1C. Very similar degradation patterns were observed after extended protease incubation for 16 h (data not shown). Degradation of the calcium-free homocysteine-treated recombinant fragments with trypsin also resulted in higher protease susceptibilities for all three fragments as compared with the non-treated calcium-free controls (data not shown; chymotrypsin was not used in these experiments).

Degradation products of homocysteine-treated fragments, which were more susceptible to either trypsin or chymotrypsin as compared with the non-treated controls, were further analyzed by N-terminal sequencing and are summarized in TABLE THREE and Fig. 6. In general, sites rendered susceptible to proteolytic degradation were found in almost all domains contained in rF1B, rF1C, and rF1D. Most sensitive sites are located in loop 4 of the cbEGF domains between cysteine residues 5 and 6 (cysteine residues of an individual cbEGF domain are numbered here as 1–6). Some sensitive sites were also found in loop 1 (between cysteines 1 and 2) and loop 2 (between cysteines 2 and 3) of various cbEGF domains as well as in various loops of the 8-Cys/TB domain 3. These data demonstrate that modification of the recombinant proteins with homocysteine results in structural changes throughout the proteins, which are sufficient to enhance their susceptibility for trypsin and chymotrypsin. In addition, several non-typical cleavage sites primarily with chymotrypsin and occasionally with trypsin were observed. These sites are almost exclusively located in close vicinity to cysteine residues (Table III and Fig. 6). These data strongly indicate that new recognition sites for chymotrypsin and trypsin were generated by covalent homocysteine modification of a number of cysteine residues in the recombinant fibrillin-1 fragments.

Taken together, this experimental set of data further support the concept that homocysteine modifies the structure of all three fragments of fibrillin-1 in that way that a number of epitopes in 8-Cys/TB and cbEGF domains become more accessible to proteases. Chymotrypsin and trypsin are used here as biochemical tools, and they do not represent physiological proteases for fibrillin-1 in extracellular matrices. However, we suggest that the structural and functional changes of fibrillin-1 induced by homocysteine are sufficient to render the protein susceptible to proteolytic attack and degradation by physiological relevant proteases in tissues. Such a mechanism may act in addition to other mechanisms suggested, including the reduction of fibrillin-1 deposition into the matrix under low cysteine conditions (32). Because potential homocysteine modification takes place in the connective tissue of individuals with homocystinuria, the secretion of the normal fibrillin-1 is likely not affected. This has been recently supported by analysis of fibroblasts from individuals with homocystinuria (34). Analysis of the consequences of elevated homocysteine levels using smooth muscle cells showed no influence on the fibrillin-1 deposition in the extracellular matrix (32). In this light it is possible that potential degradation of

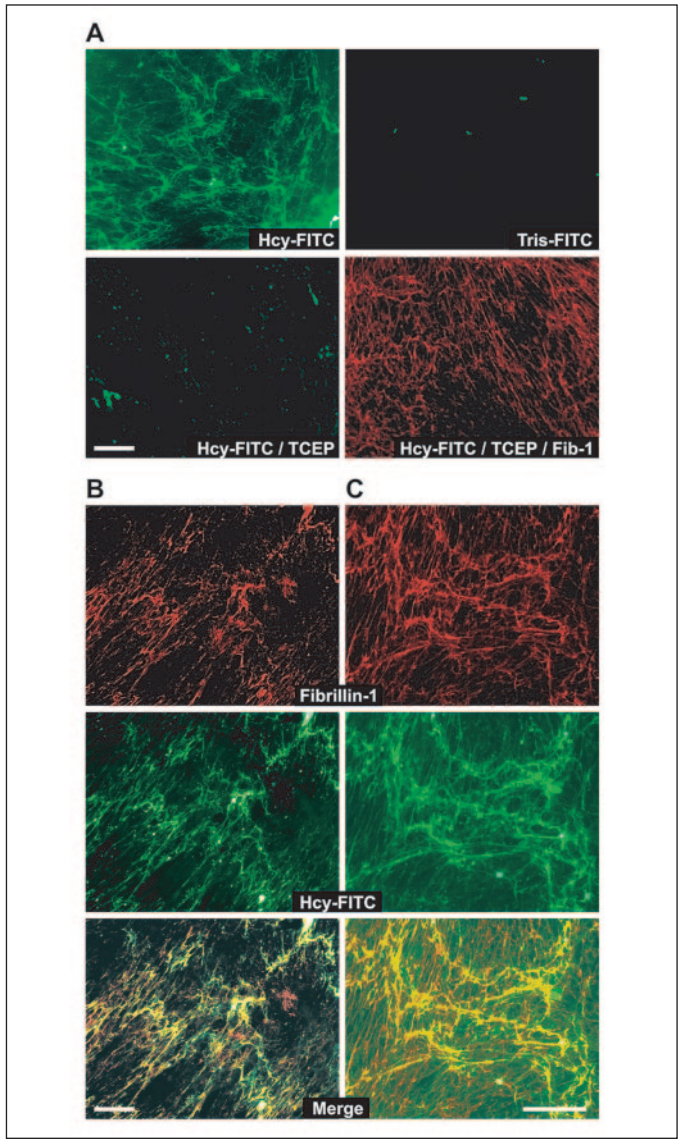

FIGURE 7. **Targeting of homocysteine to the extracellular matrix of fibroblasts.** *A*, FITC-labeled homocysteine (*Hcy-FITC*, *green signal*) was added to fibroblast cell cultures and localized by fluorescence microscopy (*left upper panel*). FITC-labeled Tris (*Tris-FITC*) was used as a control (*right upper panel*). After Hcy-FITC labeling reduction was performed with 10 mM TCEP for 30 min (*lower panels*). The absence of the green signal demonstrates that Hcy-FITC originally formed reducible bonds with extracellular matrix components (*left lower panel*). The fibrillin-1 network did not change after treatment with Hcy-FITC followed by reduction with TCEP (*red signal*, *right lower panel*). *B* and *C*, indirect double immunofluorescence was performed 3 days (*B*) or 4 days (*C*) after cell seeding with specific antibodies against fibrillin-1 (*red signals*) and with Hcy-FITC (*green signals*). Colocalization between fibrillin-1 and Hcy-FITC is indicated by the *yellow color* in the merged images. The *bars* in A, B, and C represent 100 μm.

homocysteine-modified fibrillin-1 takes place at the level of microfibrils, which may not necessarily lead to altered or diminished microfibrillar networks in the extracellular matrix. Proteolytic cleavage sites within an existing microfibril may compromise its function over time, resulting in the clinical symptoms found in individuals with homocystinuria similar to those seen in patients with Marfan syndrome. However, in a homocysteinemic chicken model with elevated homocysteine plasma levels, reduced and disrupted microfibrils were observed (31), potentially reflecting enhanced proteolytic susceptibility in vivo.

The structural and functional changes of fibrillin-1 introduced by the treatment with homocysteine may resemble the molecular consequences of the common point mutations in Marfan syndrome, which

either replace or generate new cysteine residues. It is likely that substituted or additional cysteine residues in domains requiring stabilization by disulfide bonds lead to free reactive cysteine residues or induce disulfide bond shuffling and misfolding. Some cysteine mutations in fibrillin-1 prevent secretion of the molecules, whereas others have been shown to alter the protein structure and render the mutated cbEGF domain more susceptible to proteolysis *in vitro* (14, 42, 51, 52). In this light it is possible that pathogenetic pathways leading to Marfan syndrome and to homocystinuria share some common molecular mechanisms.

Homocysteine Modification of Fibrillin-1 Networks in Cell Cultures—To analyze whether homocysteine is able to modify the extracellular matrix of cells in culture, homocysteine was covalently labeled via the amine group with the fluorescent compound FITC (Hcy-FITC) and then added to dermal fibroblasts (Fig. 7A). Hcy-FITC labeled fibrillar extracellular structures, whereas the control compound Tris-FITC did not show extensive labeling signals. After incubation of the Hcy-FITC-labeled fibroblasts with the mildly reducing agent TCEP, Hcy-FITC was no longer detectable in the extracellular matrix (Fig. 7*A*). These results indicate that Hcy-FITC covalently modifies components in the extracellular matrix in a reducible fashion via disulfide bonds. This interpretation is in agreement with the above-described observation of newly generated recognition sites for chymotrypsin and trypsin and with observations from others demonstrating homocysteine-modified adducts of fibrillin by mass spectrometry (34). To detect whether homocysteine is able to modify fibrillin-1 in the extracellular matrix of fibroblasts, double immunofluorescence experiments were performed with Hcy-FITC and specific antibodies for fibrillin-1 (Figs. 7, *B* and *C*). Fibrillin-1 and Hcy-FITC showed significant colocalization patterns, suggesting that homocysteine has the potential to modify fibrillin-1 in extracellular matrices. Incubation with either Hcy-FITC (Fig. 7) or non-labeled homocysteine (data not shown) did not disturb the formation of the fibrillin-1 networks, which is in agreement with a previous study by Majors and Pyeritz (32). This set of data clearly support that homocysteine covalently modifies fibrillin-1, which ultimately leads to the observed structural and functional alterations described above. Such changes in fibrillin-1 could explain the overlapping clinical symptoms observed in Marfan syndrome and homocystinuria. However, both disorders are also characterized by different symptoms primarily in the central nervous and the cardiovascular systems, suggesting additional selective mechanisms. Based on the potential of homocysteine to modify fibrillin-1, we predict that other cysteine-rich and disulfide-bonded molecules in extracellular matrices or on cell surfaces are also targets for homocysteine modification. Recently, Hutchinson *et al.* (34) reported the potential of homocysteine to modify Notch1, and members of the Notch family have been suggested as candidates to mediate the specific symptoms in homocystinuria. Another candidate is fibrillin-3, a newly identified member of the fibrillin family, which is significantly expressed in brain (3, 53). Based on the high overall homology of fibrillins, it is likely that fibrillin-3 is a target for homocysteine modification.

Conclusions—In this study we demonstrate that homocysteine in concentrations found in individuals with homocystinuria can alter the secondary structure of selected recombinant fibrillin-1 fragments *in vitro*. These structural changes likely occur through covalent modification of cysteine residues in fibrillin-1 and/or disulfide bond shuffling and lead to a loss of calcium binding and significantly enhanced protease susceptibility. These structural and functional changes occur within a short period (1 day) of the experimental setup. In light of the fact that patients with homocystinuria are permanently exposed to elevated homocysteine levels, we suggest that the modifications of fibrillin-1 described here play a pivotal role in the molecular pathogenesis of this disorder. This would explain the overlapping clinical symptoms observed in homocystinuria and Marfan syndrome caused by mutations in fibrillin-1.

Acknowledgments—We thank Martina Alexander for excellent technical assistance. We are grateful to Dr. Lynn Sakai and Glen Corson for providing cDNA clone HFBN8, and to Dr. Rolf Hilgenfeld for the recombinant proteinase from the severe acute respiratory syndrome virus.

REFERENCES

1. Sakai, L. Y., Keene, D. R., and Engvall, E. (1986) *J. Cell Biol.* **103,** 2499–2509
2. Zhang, H., Apfelroth, S. D., Hu, W., Davis, E. C., Sanguineti, C., Bonadio, J., Mecham, R. P., and Ramirez, F. (1994) *J. Cell Biol.* **124,** 855–863
3. Nagase, T., Nakayama, M., Nakajima, D., Kikuno, R., and Ohara, O. (2001) *DNA Res.* **8,** 85–95
4. Mecham, R. P., and Davis, E. (1994) in *Extracellular Matrix Assembly and Structure* (Yurchenco, P. D., ed) pp. 281–314, Academic Press, Inc., New York
5. Isogai, Z., Ono, R. N., Ushiro, S., Keene, D. R., Chen, Y., Mazzieri, R., Charbonneau, N. L., Reinhardt, D. P., Rifkin, D. B., and Sakai, L. Y. (2003) *J. Biol. Chem.* **278,** 2750–2757
6. Downing, A. K., Knott, V., Werner, J. M., Cardy, C. M., Campbell, I. D., and Handford, P. A. (1996) *Cell* **85,** 597–605
7. Yuan, X., Downing, A. K., Knott, V., and Handford, P. A. (1997) *EMBO J.* **16,** 6659–6666
8. Lee, S. S., Knott, V., Jovanovic, J., Harlos, K., Grimes, J. M., Choulier, L., Mardon, H. J., Stuart, D. I., and Handford, P. A. (2004) *Structure* (*Camb*) **12,** 717–729
9. Handford, P. A., Mayhew, M., Baron, M., Winship, P. R., Campbell, I. D., and Brownlee, G. G. (1991) *Nature* **351,** 164–167
10. Reinhardt, D. P., Mechling, D. E., Boswell, B. A., Keene, D. R., Sakai, L. Y., and Bächinger, H. P. (1997) *J. Biol. Chem.* **272,** 7368–7373
11. Ashworth, J. L., Murphy, G., Rock, M. J., Sherratt, M. J., Shapiro, S. D., Shuttleworth, C. A., and Kielty, C. M. (1999) *Biochem. J.* **340,** 171–181
12. McGettrick, A. J., Knott, V., Willis, A., and Handford, P. A. (2000) *Hum. Mol. Genet.* **9,** 1987–1994
13. Reinhardt, D. P., Ono, R. N., Notbohm, H., Müller, P. K., Bächinger, H. P., and Sakai, L. Y. (2000) *J. Biol. Chem.* **275,** 12339–12345
14. Vollbrandt, T., Tiedemann, K., El Hallous, E., Lin, G., Brinckmann, J., John, H., Bätge, B., Notbohm, H., and Reinhardt, D. P. (2004) *J. Biol. Chem.* **279,** 32924–32931
15. Tiedemann, K., Bätge, B., Müller, P. K., and Reinhardt, D. P. (2001) *J. Biol. Chem.* **276,** 36035–36042
16. Jensen, S. A., Reinhardt, D. P., Gibson, M. A., and Weiss, A. S. (2001) *J. Biol. Chem.* **276,** 39661–39666
17. Reinhardt, D. P., Sasaki, T., Dzamba, B. J., Keene, D. R., Chu, M. L., Göhring, W., Timpl, R., and Sakai, L. Y. (1996) *J. Biol. Chem.* **271,** 19489–19496
18. Handford, P. A., Downing, A. K., Rao, Z., Hewett, D. R., Sykes, B. C., and Kielty, C. M. (1995) *J. Biol. Chem.* **270,** 6751–6756
19. Whiteman, P., Downing, A. K., Smallridge, R., Winship, P. R., and Handford, P. A. (1998) *J. Biol. Chem.* **273,** 7807–7813
20. Reinhardt, D. P., Keene, D. R., Corson, G. M., Pöschl, E., Bächinger, H. P., Gambee, J. E., and Sakai, L. Y. (1996) *J. Mol. Biol.* **258,** 104–116
21. Glanville, R. W., Qian, R. Q., McClure, D. W., and Maslen, C. L. (1994) *J. Biol. Chem.* **269,** 26630–26634
22. Smallridge, R. S., Whiteman, P., Doering, K., Handford, P. A., and Downing, A. K. (1999) *J. Mol. Biol.* **286,** 661–668
23. Knott, V., Downing, A. K., Cardy, C. M., and Handford, P. (1996) *J. Mol. Biol.* **255,** 22–27
24. Pyeritz, R. E. (2000) *Annu. Rev. Med.* **51,** 481–510
25. Collod-Beroud, G., Le Bourdelles, S., Ades, L., Ala-Kokko, L., Booms, P., Boxer, M., Child, A., Comeglio, P., De Paepe, A., Hyland, J. C., Holman, K., Kaitila, I., Loeys, B., Matyas, G., Nuytinck, L., Peltonen, L., Rantamaki, T., Robinson, P., Steinmann, B., Junien, C., Beroud, C., and Boileau, C. (2003) *Hum. Mutat.* **22,** 199–208
26. Robinson, P. N., Booms, P., Katzke, S., Ladewig, M., Neumann, L., Palz, M., Pregla, R., Tiecke, F., and Rosenberg, T. (2002) *Hum. Mutat.* **20,** 153–161
27. Skovby, F., and Kraus, J. P. (2002) in *Connective Tissue and its Heritable Disorders* (Royce, P. M., and Steinmann, B., eds) pp. 627–650 Wiley-Liss, Inc., New York
28. Ueland, P. M., Refsum, H., and Brattstrom, L. (1992) in *Atherosclerotic Cardiovascular Disease, Hemostasis, and Endothelial Function* (Francis, R. B. J., ed.) pp. 183–236, Marcel Dekker, Inc., New York
29. Refsum, H., Ueland, P. M., Nygard, O., and Vollset, S. E. (1998) *Annu. Rev. Med.* **49,** 31–62

30. Pyeritz, R., and Dietz, H. (2002) in *Connective Tissue and Its Heritable Disorders* (Royce, P. M., and Steinmann, B., eds) pp. 585–626, Wiley-Liss, Inc., New York
31. Hill, C. H., Mecham, R., and Starcher, B. (2002) *J. Nutr.* **132,** 2143–2150
32. Majors, A. K., and Pyeritz, R. E. (2000) *Mol. Genet. Metab.* **70,** 252–260
33. Lentz, S. R., and Sadler, J. E. (1991) *J. Clin. Investig.* **88,** 1906–1914
34. Hutchinson, S., Aplin, R. T., Webb, H., Kettle, S., Timmermans, J., Boers, G. H., and Handford, P. A. (2005) *J. Mol. Biol.* **346,** 833–844
35. Corson, G. M., Chalberg, S. C., Dietz, H. C., Charbonneau, N. L., and Sakai, L. Y. (1993) *Genomics* **17,** 476–484
36. Lin, G., Tiedemann, K., Vollbrandt, T., Peters, H., Bätge, B., Brinckmann, J., and Reinhardt, D. P. (2002) *J. Biol. Chem.* **277,** 50795–50804
37. Duerre, J. A., and Miller, C. H. (1966) *Anal. Biochem.* **17,** 310–315
38. Sedlak, J., and Lindsay, R. H. (1968) *Anal. Biochem.* **25,** 192–205
39. Provencher, S. W., and Glockner, J. (1981) *Biochemistry* **20,** 33–37
40. van Stokkum, I. H., Spoelder, H. J., Bloemendal, M., van Grondelle, R., and Groen, F. C. (1990) *Anal. Biochem.* **191,** 110–118
41. Reinhardt, D. P., Gambee, J. E., Ono, R. N., Bächinger, H. P., and Sakai, L. Y. (2000) *J. Biol. Chem.* **275,** 2205–2210
42. Whiteman, P., and Handford, P. A. (2003) *Hum. Mol. Genet.* **12,** 727–737
43. Julenius, K., Molgaard, A., Gupta, R., and Brunak, S. (2005) *Glycobiology* **15,** 153–164
44. Ritty, T. M., Broekelmann, T., Tisdale, C., Milewicz, D. M., and Mecham, R. P. (1999) *J. Biol. Chem.* **274,** 8933–8940
45. Adam, S., Goehring, W., Wiedemann, H., Chu, M. L., Timpl, R., and Kostka, G. (1997) *J. Mol. Biol.* **272,** 226–236
46. Jensen, S. A., Corbett, A. R., Knott, V., Redfield, C., and Handford, P. A. (2005) *J. Biol. Chem.* **280,** 14076–14084
47. Kettle, S., Yuan, X., Grundy, G., Knott, V., Downing, A. K., and Handford, P. A. (1999) *J. Mol. Biol.* **285,** 1277–1287
48. Ritty, T. M., Broekelmann, T. J., Werneck, C. C., and Mecham, R. P. (2003) *Biochem. J.* **375,** 425–432
49. Marson, A., Rock, M. J., Cain, S. A., Freeman, L. J., Morgan, A., Mellody, K., Shuttleworth, C. A., Baldock, C., and Kielty, C. M. (2005) *J. Biol. Chem.* **280,** 5013–5021
50. Reinhardt, D. P., Ono, R. N., and Sakai, L. Y. (1997) *J. Biol. Chem.* **272,** 1231–1236
51. Schrijver, I., Liu, W., Brenn, T., Furthmayr, H., and Francke, U. (1999) *Am. J. Hum. Genet.* **65,** 1007–1020
52. Booms, P., Tiecke, F., Rosenberg, T., Hagemeier, C., and Robinson, P. N. (2000) *Hum. Genet.* **107,** 216–224
53. Corson, G. M., Charbonneau, N. L., Keene, D. R., and Sakai, L. Y. (2004) *Genomics* **83,** 461–472
54. Pereira, L., D'Alessio, M., Ramirez, F., Lynch, J. R., Sykes, B., Pangilinan, T., and Bonadio, J. (1993) *Hum. Mol. Genet.* **2,** 961–968

Modification of the Structure and Function of Fibrillin-1 by Homocysteine Suggests a Potential Pathogenetic Mechanism in Homocystinuria

Dirk Hubmacher, Kerstin Tiedemann, Rainer Bartels, Jürgen Brinckmann, Tillman Vollbrandt, Boris Bätge, Holger Notbohm and Dieter P. Reinhardt

J. Biol. Chem. 2005, 280:34946-34955.
doi: 10.1074/jbc.M504748200 originally published online August 11, 2005
